4-2022

Short-Term 2D And 3D Geomorphic Change Detection At A Public Park On Lake Michigan Using UAS Remote Sensing Techniques

Scott Patrick Fitzgerald
Western Michigan University

SHORT-TERM 2D AND 3D GEOMORPHIC CHANGE DETECTION AT A PUBLIC PARK ON LAKE MICHIGAN USING UAS REMOTE SENSING TECHNIQUES

Scott P. Fitzgerald, M.S.

Western Michigan University, 2022

The high-water level of Lake Michigan (LM) in the past few years has led to significant periods of erosion and increased the risk to private property owners on the coast. To cope with this, many property owners on the coast of LM have constructed coastal protections, some opting for seawalls. Previous studies have assessed the effects of seawalls but disagreed on their impacts, and only laboratory studies were able to establish their range of influence. Using a different method to study their effects will be pertinent to understanding them.

This research aims to use a higher temporal and spatial resolution approach, Unoccupied Aircraft System (UAS) aerial image collection with Structure from Motion (SfM) image processing, than previous studies to examine the effects of a seawall on an adjacent Lake Michigan beach. Previous studies have relied on satellite imagery or visual observation to conclude results. However, satellite data does not provide 3-dimensional data and are too low a resolution for repeat observation, and visual inspection can introduce bias.

Over 9 months and 18 aerial surveys of a public park on Lake Michigan, 2D and 3D changes in the beach and dune were recorded. Using the extent of shorelines, two sites were set up: site 1 under influence of the seawall and site 2, under no influence. Measurements were made between shoreline positions to create the shoreline average difference variable. A t-test of unequal variances was used to determine if site 1 had more erosion than site 2 ($p < .50$). For 3D data, elevation change values were gathered using raster differencing. There were significant

negative elevation changes in many parts of the dune (<-2.5 ft). However, due to issues with the SfM-MVS method, the dune covered in heavy vegetation, elevation changes could not be obtained. Thus, it is difficult to discern if the changes are brought on the adjacent seawall or if other factors such as tourist movement or heavy storms could have caused the negative elevation changes.

SHORT-TERM 2D AND 3D GEOMORPHIC CHANGE DETECTION AT A PUBLIC PARK ON LAKE MICHIGAN USING UAS REMOTE SENSING TECHNIQUES

by

Scott P. Fitzgerald

A thesis submitted to the Graduate College
in partial fulfillment of the requirements
for the degree of Master of Science
Geography
Western Michigan University
April 2022

Thesis Committee:

Adam J. Mathews, Ph.D., Chair
Lisa M. DeChano-Cook, Ph.D.
Chansheng He, Ph.D.

ACKNOWLEDGMENTS

My first interaction with the idea of science came about from Carl Sagan's TV show *Cosmos: A Personal Voyage* (1980). I start this acknowledgment section off with a quote that stuck with me for some time in a show that initially sparked my interest in science, also due to its particular relevance to the subject of my research: "The surface of the Earth is the shore of the cosmic ocean. On this shore, we've learned most of what we know. Recently, we've waded a little way out, maybe ankle-deep, and the water seems inviting (Sagan et al., 1980)."

To my research assistant, thank for you coming to the beach with me each week. Data collection would not have happened without you. To Autumn, thank you for making a bad living situation into a habitable one: "THE PROPHECY IS TRUE!". To Bean, my adopted cat, thank you for walking across my keyboard when I was working too hard.

To my professors, I would not have found this topic if it were not for you. All of you had strong support from the conception of the project, emphasizing the value and practicality this project could have. That flattery only made me work harder and gave me the will I needed to complete a project of this magnitude.

Special thanks to: Peter Colovos, you were so kind and quick to give permission to use HPB. Ken Bates, for giving me a key to the park and always available for a chat. To all the visitors of HPB, for being understanding when half your beach was closed off for a few hours every other week.

Scott P. Fitzgerald

TABLE OF CONTENTS

LIST OF TABLES

LIST OF FIGURES

INTRODUCTION

Many hydrologic processes drive the geomorphology of Lake Michigan's shoreline. Lake Michigan's water level has reached above-average levels for every month of the year since 2015 (US Army Corps of Engineers, 2020). The water level in Lake Michigan is inches away from breaking the known record, initially set in 1985-1986 (see Figure 1; US Army Corps of Engineers, 2020). Due to the high-water level, Michigan's Department of Environment, Great Lakes, and Energy (EGLE) has characterized most of Michigan's western shoreline as high risk for erosion (EGLE, 2020a). Shoreline protections are an attempt by private landowners along the shore to cease the erosion and loss of their property. Between October 2019 and July 2020, EGLE approved 1,771 permits to construct permanent shoreline protections (House, 2020).

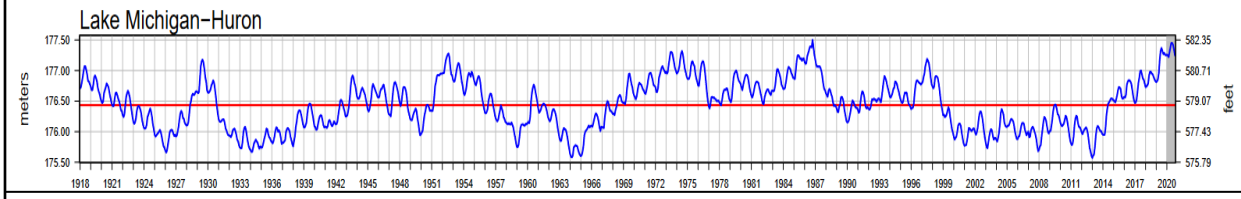

Figure 1. *Historical water level data of the Lake Michigan-Huron basin from 1918 to 2020. The red line shows the long-term average annual and in blue shows the monthly mean water level (U.S. Army Corps of Engineers, 2020).*

Many shoreline protections exist, classified as 'hard' or 'soft' (National Research Council, 1995). Hard shore protections include bulkheads, seawalls, breakwaters, revetments, jetties, and groins (National Research Council, 1995). Soft shore protection involves nonpermanent structures; beach nourishment is a soft protection type that adds sand to a beach (National Research Council, 1995). Adding sand to the beach will enlarge the reservoir, pushing the beach seaward or lakeward; a more extensive beach can better dissipate wave energy than a smaller one (National Research Council, 1995). Other 'soft' protections involve adding deep-rooted plants or unmowed vegetation to decrease erosion (EGLE, 2020b). Hard shoreline

protections, such as seawalls, can negatively impact the lake's fishery, wildlife, and water quality. Moreover, seawalls can affect adjacent beaches with the end-wall effect (EGLE, 2020b; Balaji et al., 2017; Basco et al., 2006; McDougal et al., 1987; Walton & Sensabaugh, 1978).

LITERATURE REVIEW

The Lake Michigan-Huron basin has long been an area of study, from the geologic formation due to glaciers to more recently focused on the water level (Volpano et al., 2020; Theuerkauf et al., 2019; Fraser et al., 1990). The water level of the Lake Michigan-Huron basin is influenced by rainfall, run-off, discharge, evaporation, and evapotranspiration (Fraser et al., 1990). The history of its water level has been established by collecting sediment cores and many analytical methods for the past 12,000 years (Steven et al., 1994). Water levels facilitating the geomorphic change of the shoreline have been well documented. Remote sensing (RS) and geographic information systems (GIS) have recently been used to aid coastal research (Volpano et al., 2020; Zimmerman et al., 2020; Pagán et al., 2019; Theuerkauf et al., 2019; Conlin et al., 2018; Westoby et al., 2018; Balaji et al., 2017; Cook, 2017; Sturdivant et al., 2017; Papakonstantinou et al., 2016; Rossi et al., 2016; Vericat et al., 2016; Javernick et al., 2014; Mancini et al., 2013; James & Quinton, 2012). Repeatable satellite imagery has a lengthy catalog dating back to when Landsat 1 was launched in 1972. The 30-meter spatial resolution of the satellite is not high enough spatial resolution to observe precise changes in the shoreline, daily, monthly, or yearly, and most likely decadal (Carrivick et al., 2016).

Many studies have been done regarding geomorphic change due to shoreline protections (Balaji et al. 2017; Lin et al. 2014; Miles et al. 2001; MacIntosh & Anglin 1988; Komar & McDougal 1988), with only a few utilizing RS and GIS to obtain results (Balaji et al. 2017; Lin

et al. 2014). However, a few studies have found that coastal structures do not significantly affect beach profiles (Kraus & McDougal, 1996; Plant & Griggs, 1992). On the Northwestern U.S. coast, Komar and McDougal (1988) did not prove that structures induce erosion of adjacent properties during their study due to a lack of strong erosion events. Plant and Griggs (1992) found a lack of severe erosion events in the beach adjacent to a seawall on the Californian coast. However, their conclusions were primarily visual observations, suggesting continuous monitoring and three-dimensional measurements for future studies (Plant & Griggs, 1992).

Walton and Sensabaugh (1978) did field observations post-hurricane Eloise of two beaches adjacent to seawalls; excessive erosion on the beaches was attributed to the adjacent seawall. Lin et al. (2014) studied the nearshore environment before and after constructing a coastal structure in the Lake Michigan-Huron basin using both RS and in-situ observations. They found negative impacts on bluff stability due to erosion on the beach adjacent to the newly built structure (Lin et al., 2014). Balaji et al. (2017), on the Indian coast, found that the construction of a coastal structure resulted in landward erosion of approximately 65 feet (20 m) on the beach downdrift of the seawall. Attempts have been made by researchers to determine the influence range of an adjacent seawall to no success. However, researchers in controlled laboratory studies have concluded that the effect on adjacent beaches is a function of the seawall length (McDougal et al., 1987).

A seawall can protect a beach from erosion occurring at that beach because it redirects the wave energy away from hitting the beach (Balaji et al., 2017). However, that wave energy must end up somewhere – typically causing more erosion down-drift of the seawall, producing the end-wall effect (Balaji et al., 2017; Basco et al., 2006; McDougal et al., 1987; Walton & Sensabaugh, 1978). Because the purpose of a seawall has an unintended consequence for

beaches in relation, their effects must be studied to know the potential outcomes before constructing them.

Recent research on geomorphic change due to shoreline protections has primarily involved RS and GIS (Balaji et al., 2017; Lin et al., 2014). Repeat data collection of coastal environments commonly involve survey-grade, high accuracy (both horizontal and vertical) Global Navigation Satellite System (GNSS) equipment (i.e. Real-Time Kinematic or RTK) (McKenna & Farrell, 2014; Harley et al., 2011; Yates et al., 2009; Ruggerio et al., 2005), total station (Gibbs et al., 2001), terrestrial laser scanning (TLS) (Pietro et al., 2008; laser scanning otherwise known as light detection and ranging, simply lidar), and airborne laser scanning (ALS) (Sallenger et al., 2003). These are valuable methods to monitor coastal environments but do present disadvantages when observing short term changes, needing a high resolution, . For example, remote sensing from satellite imagery is helpful to monitor geomorphic change when the time between observation intervals is yearly to decadal because it cannot distinguish small-scale changes due to its low spatial resolution (Papakonstantinou et al., 2016). Likewise, techniques involving lidar (TLS and ALS) require expensive equipment and are unavailable in many areas (Conlin et al., 2018; Papakonstantinou et al., 2016). In addition, RTK surveys can fail to determine small-scale features in 3D (Ruggiero et al., 2005). None of these methods can provide both two-dimensional and three-dimensional data alone and frequent observations can be costly. While these are valued methods to provide insightful results to their respective application, there use may have to be supplemented with other methods to provide insightful results. This study explores a relatively new RS method to determine its applicability to study the effects of seawall on an adjacent beach.

A low-cost and high-resolution method to monitor geomorphic change has emerged (Conlin et al., 2018; Carrivick et al., 2016; Mathews & Jensen, 2012). Structure from Motion-Multiview Stereo (SfM-MVS) photogrammetry creates three-dimensional topographic data and two-dimensional orthomosaics from a series of overlapping images. The relatively low cost of this method stems from its ability to perform well with consumer-grade cameras (Carrivick et al., 2016). Cameras can be attached to a variety of platforms: unoccupied aircraft systems (UAS) or drones (Turner et al., 2016; Mathews & Jensen, 2013; Dunford et al., 2009), blimps (Vericat et al., 2009), kites (Westoby et al. 2015; Smith et al., 2009), telescopic poles (Rossi et al., 2016; Mathews & Jensen, 2012; Plets et al. 2012), and occupied aircraft (Javernick et al., 2014; James & Varley, 2012) have been utilized to collect images for use in SfM-MVS. Conlin et al. (2018) suggest that UAS platforms and SfM-MVS image processing can obtain the most accurate results in coastal environments compared to other SfM-MVS methods mentioned. The resulting SfM-MVS point cloud needs to be georeferenced to get measurements; the point cloud can be georeferenced directly or indirectly. Indirect georeferencing is done with ground control points; a minimum of three are required, with XYZ coordinates. Researchers have concluded the optimal configuration to maximize accuracy for ground control points (GCPs) on coastal environments are in the corners of the study site, at both high and low elevations, and with sufficient cross-shore and alongshore coverage (Zimmerman et al., 2020; Westoby et al., 2018). Alternatively, a direct georeference can be achieved when the camera positions at the time of imaging are derived with an RTK and inertial measurement unit (IMU) (Turner et al., 2014; Tsai et al., 2010).

Many studies have utilized UAS-SfM-MVS (hereby abbreviated to UAS-SfM) to observe geomorphic change (Turner et al., 2016; Theuerkauf et al., 2019; Conlin et al., 2018; Cook,

2017; Mancini et al., 2013; Pagán et al., 2019; Zimmerman et al., 2020). Studies suggest that UAS-SfM is comparable in accuracy to commonly used methods, such as TLS (Mancini et al., 2013; Sturdivant et al., 2017; Cook, 2017; Oúedraogo et al., 2014; Favalli et al., 2012; Thoeni et al., 2014; James & Quinton, 2013; Westoby et al., 2012). UAS-SfM cannot produce accurate surface elevations in densely vegetated areas; this can be improved by taking oblique images (Sturdivant et al., 2017). This problem does not occur in sand due to the lack of vegetation (Sturdivant et al., 2017). UAS-SfM data produce higher resolution and denser point clouds than other surveying methods in sandy beach areas (Sturdivant et al., 2017). UAS-SfM has the capability to provide new insights towards geomorphic change studies due to its low cost, high precision 3D point clouds, visual reflectance data, and its capability for rapid deployment (Sturdivant et al., 2017).

Objectives

The broad research question for this study is: Do seawalls increase erosion on adjacent beaches, and what is the distance range of their influence? This question will be answered through the following research objective (and two-subobjectives):

1) Examine coastal geomorphic change at Hagar Park/Beach, Michigan by:
    a) comparing seawall and non-seawall two-dimensional (2D) shoreline position over time, and
    b) comparing seawall and non-seawall erosional three-dimensional (3D; volumetric) change over time.

METHODS

Study Site

The study site is in southwestern Michigan on the shore of Lake Michigan, specifically Hagar Park/Beach (HPB), located in Hagar Township (Figures 2 and 3). The park is managed by Hagar Township who, granted permission to conduct this study. Permission was readily granted due to the concerns of erosion by township administrators. The study site is downdrift to a seawall located on private property and cement wave breakers located on park property (only the public park will be under observation due to access and permissions). This site was visited bi-weekly on Wednesdays from March 2021 to November 2021 to observe geomorphic change. This site was selected due to its adjacency due to the coast parallel seawall, the easy (and continual) access, and the park is publicly owned. It was essential to have this study at a park because private property owners would be unlikely to grant permission (or give concurrent permission) if a possible outcome of this study sheds a negative light on the impact of seawalls. The study area was split into two sites: Site 1 is under the most influence of the seawall wave redirection. Site 2, farther north on HPB, is under less influence from the seawall (Figure 4). The boundary between Site 1 and 2 was placed 205 feet away from the seawall after digitizing the shoreline positions and visually observing where the shorelines begin to experience minor variation and spread in extent.

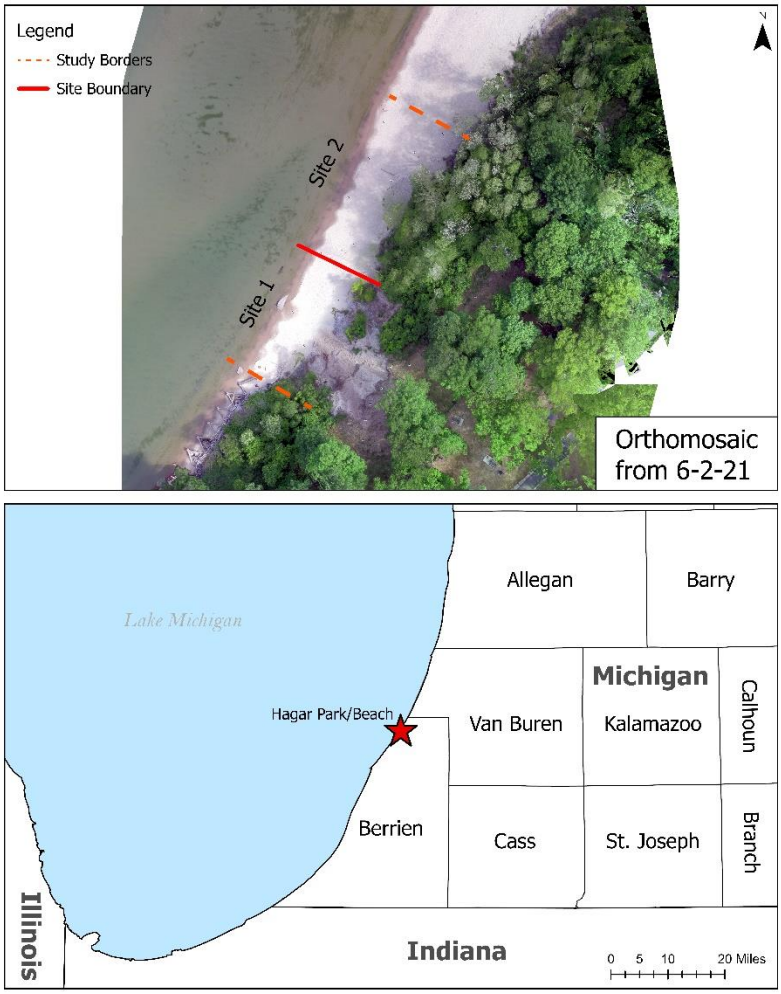

Figure 2. *Location of the study site in Hagar Township.*

Figure 3. *Hagar Park/Beach. Photographed by UAS on September 26th, 2020.*

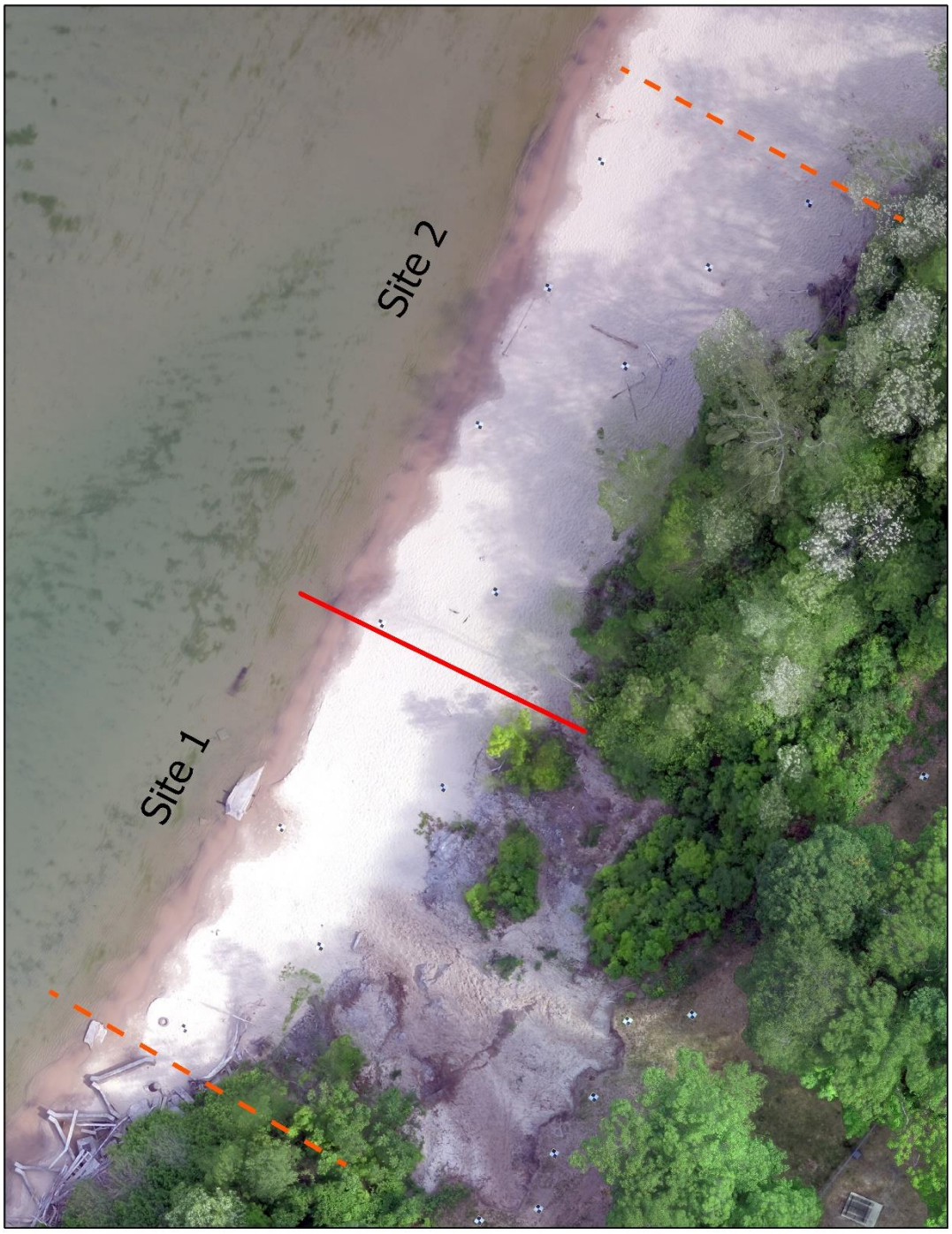

Figure 4. *Aerial view of the study area, 6-2-21. The study area is divided into two sites, at 205 feet from the seawall, by the red line to compare the shorelines differences. The southern portion of the beach is Site 1 (closest to the seawall), and the Northern part is Site 2.*

Aerial Image Data to Observe Geomorphic Change

Aerial images were collected using an off-the-shelf DJI Inspire 1 UAS with an integrated camera and gimbal system (Figure 5). Aerial images were gathered on two automated flight paths with 90% overlap with the camera at an 80-degree angle on the first path and 70-degrees on the second to improve keypoint matching and the resulting outputs (Mancini et al., 2016; Mathews & Jensen, 2013; Dandois & Ellis, 2010). Camera settings were adjusted to maintain high within-image contrast (Pix4D, n.d). A flying height altitude of 45 meters (~148 ft) above ground-level was used throughout the study to ensure a similar spatial resolution for each data collection and significant overlap between images (at least ten overlapping images) to ensure adequate keypoint matching on bare sand (Zimmerman et al., 2020; Carrivick et al., 2016; Mancini et al., 2016) and to increase the density of the resulting point cloud (Mathews & Jensen, 2013). Propeller Aeropoints were used as GCPs to indirectly georeference the images, orthomosaic, and point cloud (Carrivick et al. 2016). GCPs were placed on both high (on the dune) and low (the beach face) areas and spatially distributed throughout the study site following Zimmerman et al. (2020) and Westoby et al. (2018) methods. GCPs were placed in the corners of the study area. However, one corner could not be used due to its location in heavy vegetation; a viable alternative was chosen (Zimmerman et al., 2020; James & Robson, 2012). A stratified placement of GCPs was utilized with one-fifth (9 m) to one-tenth (4.5 m) spacing between GCPs (Harwin & Lucieer, 2012) of the flight altitude (=45 m) was utilized for the GCPs to procure sufficient cross-shore distribution (Zimmerman et al., 2020) and avoid clustering to decrease the root mean square error (RMSE) and mean absolute error (MAE) (Javernick et al., 2014; James & Robson, 2012). GCPs with substantial horizontal and vertical errors were removed to improve the total error (Vericat et al., 2016). A minimum of three GCPs is needed to georeference a point

cloud. If GCPs are removed to below three, the entire survey will be removed. Positions of the camera at the time of capture will be used to process these data but ultimately overwritten by the indirect georeference. Pix4Dmapper and Pix4Dcloud software created digital surface models (DSMs) and orthomosaics, multiple overlapping aerial view photos 'stitched' together to form one cohesive photo of the study area. An informational table describes survey conditions and collection amounts for each date below (Table 1).

Figure 5. *DJI Inspire 1 UAS with camera and gimbal system used to photograph Hagar Park/Beach (Simon, 2015).*

Table 1. Weather conditions of each UAS data collection

Date	Weather Conditions	# of GCPs	# of Flights	# of Images	Used in Study	If no, why?
3-3-21	Sunny	20	3	253	No	Snow/Ice accumulation
3-17-21	Sunny	20	3	683	Yes	---
4-5-21	Partly cloudy	20	3	630	Yes	---
4-21-21	Partly cloudy	20	2	411	Yes	---
5-5-21	Sunny	19	2	389	Yes	---
5-19-21	Cloudy	18	3	529	No	Substantial GCP vertical errors
6-2-21	Sunny	20	2	396	Yes	---
6-16-21	Sunny	18	2	318	No	Substantial GCP vertical errors
7-7-21	Sunny	19	2	320	No	Georeferencing errors
7-28-21	Sunny	18	3	585	Yes	---
8-4-21	Sunny	16	2	316	No	Substantial GCP vertical errors – Propeller failure to reprocess
8-18-21	Partly cloudy	17	2	344	Yes	---
9-1-21	Sunny	15	2	344	Yes	---

Table 1 – continued

9-15-21	Sunny	15	2	346	Yes	---
10-6-21	Cloudy	15	2	412	Yes	---
10-20-21	Sunny	17	2	346	Yes	---
11-3-21	Sunny	16	2	326	Yes	---
11-17-21	Cloudy	16	2	389	Yes	---

UAS Operation

During UAS flight, all rules of Part 107 CFR 14 put forth by the Federal Aviation Administration (FAA) were followed. At no point did flight happen over another person not part of the flight crew. Signs and cones were placed around the study area to inform park patrons of the study. The study area is in Class G airspace, underneath Class E airspace, which begins at 700 feet above ground level (AGL). I did not need air traffic control (ATC) authorization to operate a UAS because flight will never exceed the FAAs limit of UAS flight over 400 feet AGL. Likewise, Hagar Park/Beach is not within a five-mile radius of controlled airspace; the nearest airport (Southwest Michigan Regional Airport) is 6.17 miles away. The UAS was always in the visual observers (VO), and my visual line-of-sight (VLOS) and communication was established through a two-way radio. Further, approval for the study was granted by the Western Michigan University UAS Review Board on April 5th, 2021.

2D Methods

Orthomosaics were exported into ArcGIS Pro to digitize the position of the shoreline; identified using the high-water line (ESRI, n.d; Pagán et al., 2019). Measurements were made laterally along 56 transects perpendicular to shorelines; these transects were created using the USGS's Digital Shoreline Analysis System (DSAS) add-on to ArcMap (USGS). These measurements were made between shorelines of different dates to determine their difference, and negative values were given if the shoreline accreted and positive if the shoreline eroded.

3D Methods

DSMs were exported from Pix4Dmapper and imported into ArcGIS Pro (ESRI, n.d). The DSMs were converted to raster images using elevation as the cell value. The raster calculator tool was used to find the difference between elevation values using the following equation:

Elevation Difference = [Later date elevation raster] – [Earlier date elevation raster] *Eq.1*

(e.g., $DSM_{difference} = DSM^{11/17/21} – DSM^{3/17/21}$)

The original plan for the 3D methods was to get volumetric changes. To do this I used ArcGIS Pro's Surface Difference Tool, however, each time it was utilized the tool would fail to execute. No error message was given due to the tool never completing, the program itself would freeze. It is likely due to the point clouds created by UAS-SfM being too dense, as the tool is specifically meant for lidar datasets.

Structure-from-Motion-Multiview Stereo (SfM-MVS) Photogrammetry

SfM-MVS is a computer vision technique used to model objects and environments in 3D (Carrivick et al., 2016; Thoeni et al., 2014; Favalli et al., 2014; Ouédraogo et al., 2014; Fonstad et al., 2012; Westoby et al., 2012; James & Robson, 2012; Snavely et al., 2008). The mathematical backing of the SfM-MVS method is outside the scope of this thesis, but interested readers are referred to significant sources (Triggs et al., 2000; Hartley & Zisserman, 2003; Lowe, 2004; Snavely, 2008; Szeliski, 2011). A 3D point cloud of features in the study area was constructed using Pix4Dmapper software by taking overlapping photos at different angles and distances with the same vantage point. Using the Pix4D software, the point cloud was projected using the North American Datum (NAD) (2011) / Michigan South (ft). The method to process these collected data into digital surface models and orthomosaics is shown in Figure 6. GCP data and aerial imagery was used to generate a sparse point cloud. The GCP data were uploaded

to Propeller's server for processing using the Propeller Correction Network. The file, downloaded from Propeller, was imported into Pix4Dmapper and each GCP was marked in at least 15 images with the GCPs visible using the software's GCP/MTP manager and basic editor. A dense georeferenced point cloud was then generated in Pix4D mapper; both an orthomosaic and LAS dataset, an industry standard format for elevation datasets, were created as outputs.

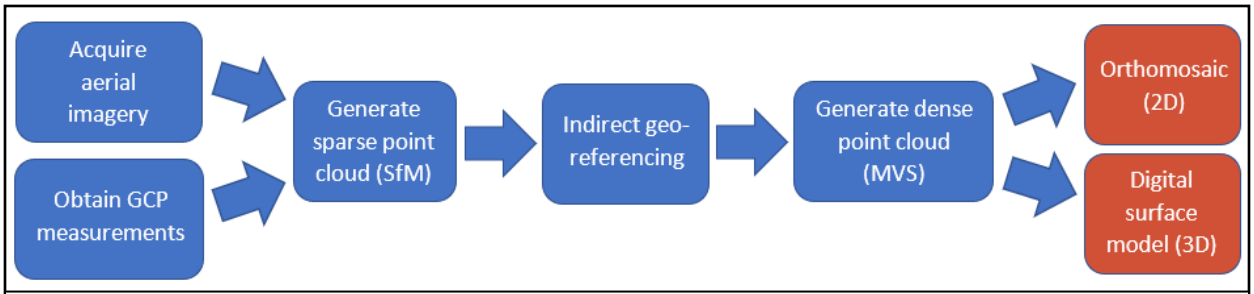

Figure 6. *SfM-MVS workflow. The flow chart used to process data into a DSMs and orthomosaics.*

RESULTS

2D Shoreline Position Analysis

The shoreline over the study duration (March 17th to November 17th) changed drastically, whether in site 1 or site 2 (Figure 7). Both locations have accretional and erosional periods. Starting on March 17th, most of site 1 is already farther landward than in site 2. A tombolo forms behind the cement foundation; however, the side facing the seawall is typically longer (Figure 7). There is some accretion between March 17th and April 7th, but most of the beach undergoes erosion, while site 2 has minimal accretion (Figure 8). The remnant of the tombolo is still there but is no longer connected to the cement foundation (Figure 7b). Between April 21st and May 5th, both sites 1 and 2 experience erosion (Figure 8). Both sites have a significant accretional period between May 5th and June 2nd (Figure 8). The tombolo is beginning to form again (Figure 7e). Between June 2nd and June 16th, there is erosion in site 1

and a mix of erosion and accretion in site 2, mainly erosion by a small margin (Figure 8). Between June 16th and July 28th, there is a majority accretion and spurts of erosion in site 1 (Figure 8). There is a significant erosional period between July 28th and August 18th, with more erosion occurring in site 2 (Figure 8). There is another significant erosional period between August 18th and September 1st, with more erosion in site 1 (Figure 8). In site 1, the shoreline is where the unvegetated dune begins; the flat beach has nearly dissipated (Figure 7i). Between September 1st and September 15th, both sites experience minimal changes in erosion and accretion; however, a majority erosion by a small margin (Figure 8). There is a switch along with site 1 between erosion and accretion, while in site 2, there is one dramatic switch (Figure 8). Between September 15th and October 6th, both sites had a massive accretion period, but site 2 experienced more accretion (Figure 8). Between October 6th and October 20th, there is significant erosion in site 1 closest to the seawall, while there is minimal accretion towards the 205-foot boundary (Figure 8). Site 2 experiences majority accretion, with one minimal spot of erosion. Between October 20th and November 11th, in site 1, there is a significant accretional period and an erosional period in site 2 (Figure 8). Between November 11th and November 17th, there is an erosional period on both sites, but more on site 1 (Figure 8).

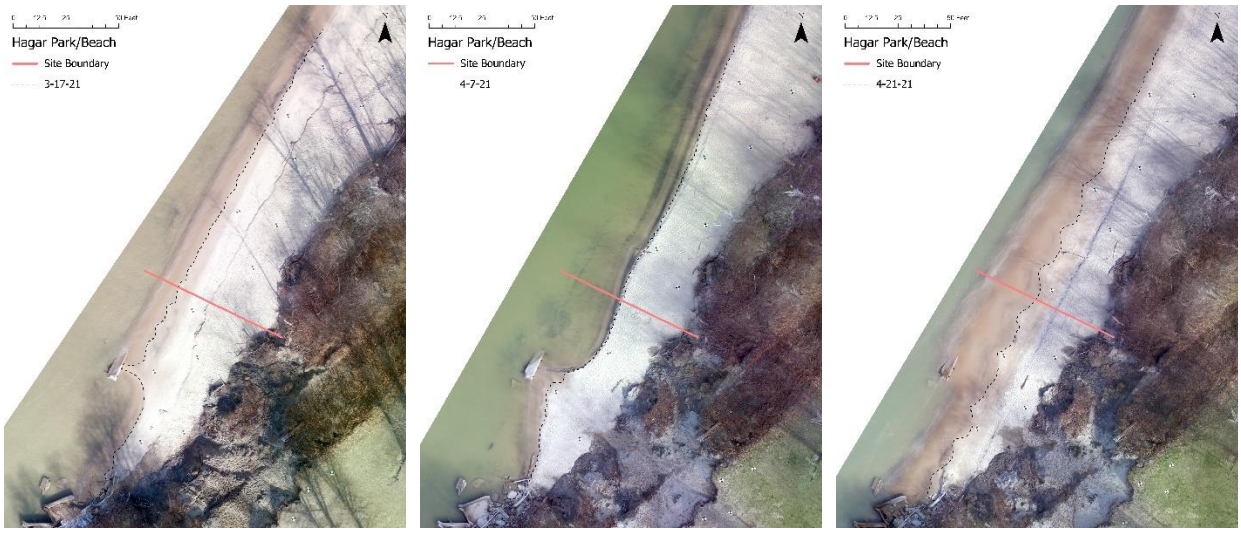

a

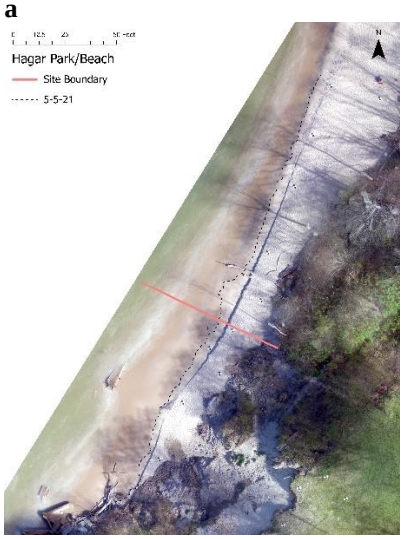

b

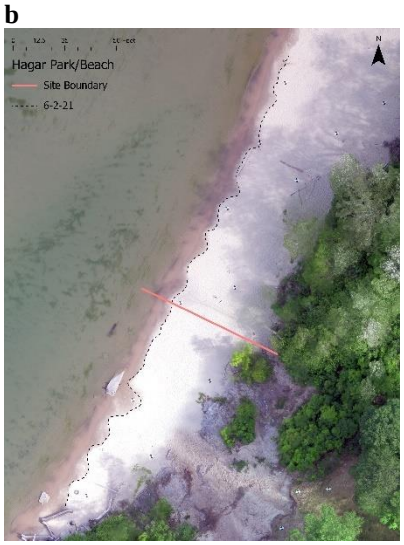

c

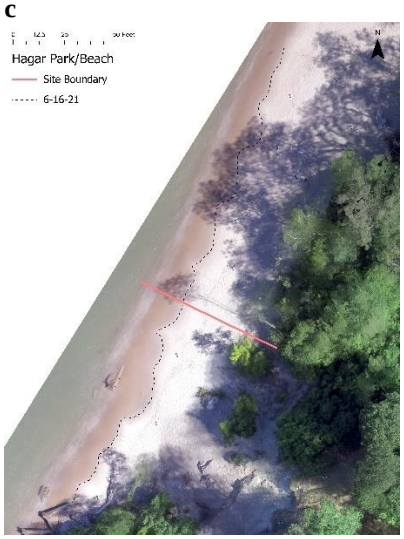

d

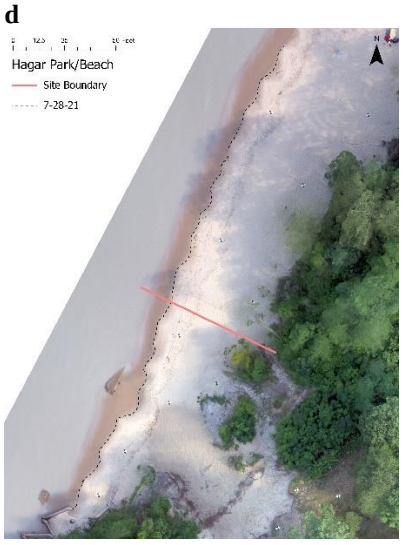

e

f

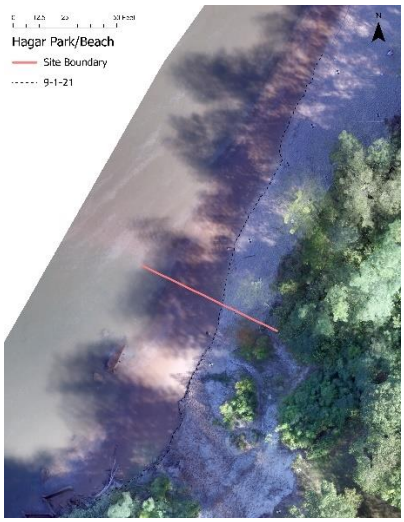

g

h

i

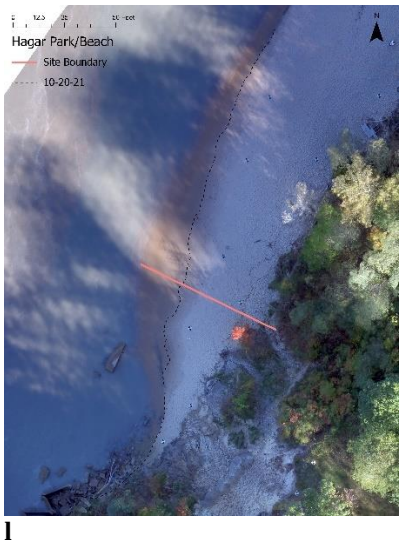

j

k

l

m **n**

Figure 7. Shoreline positions from March 17th to November 17th, 2021.

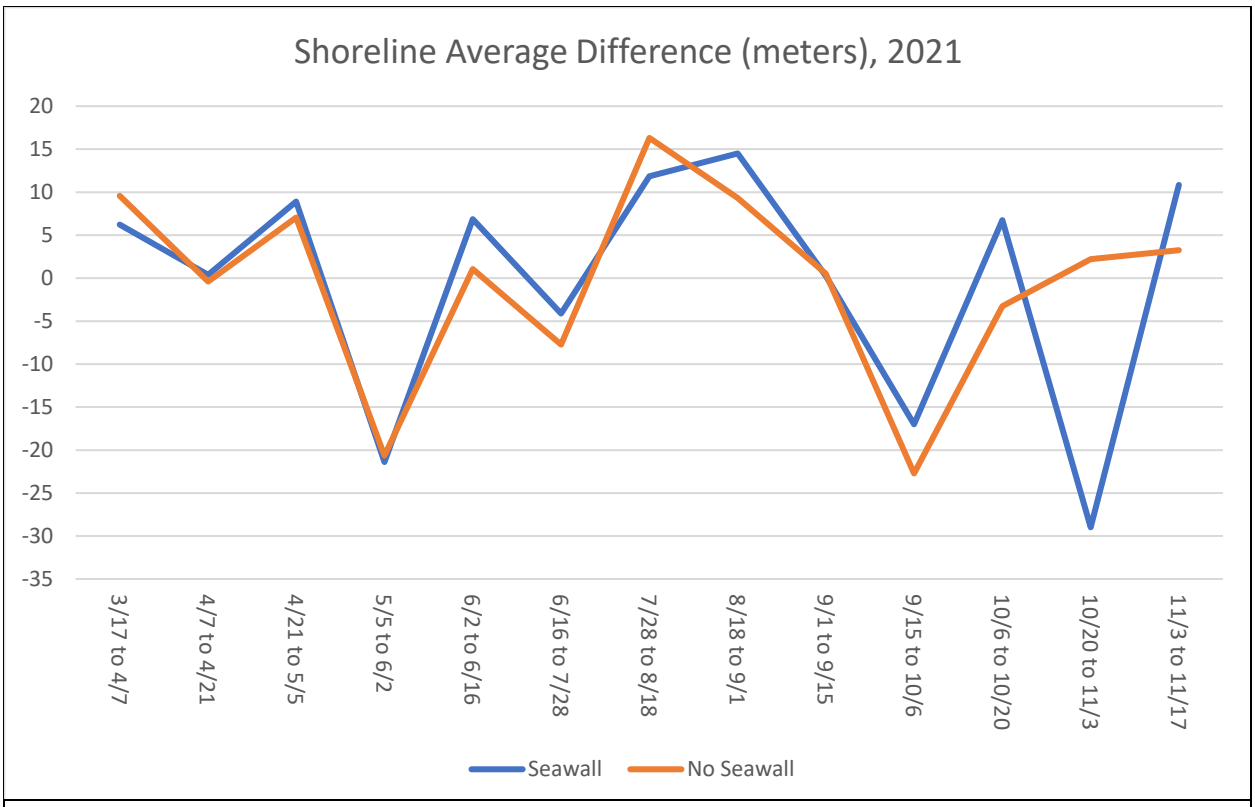

Figure 8. *Shoreline average difference between biweekly surveys. Positive values indicate erosion, and negative values indicate accretion.*

The difference between shoreline positions is relatively tiny; towards the middle of the study (June 2nd, 2021, to September 15th, 2021), the differences between shoreline positions are minimal but visually noticeable in Figure 7. Figure 9 shows the difference in the spread of the

shoreline between site 1 and 2; the shoreline in site 1 reaches a further extent in-land and out. There are different accretional and erosional periods towards the end of the study (October 6th, 2021, to November 17th, 2021). The shoreline is eroded to the beginning of the dune in Site 1 multiple times and experiences a period of accretion after. The most substantial difference between the sites' average shoreline difference is between October 20th and November 3rd when Site 1 undergoes a significant period of accretion and Site 2 experiences moderate erosion. Utilizing a t-test of unequal variances, the average shoreline difference variable from both sites was used to determine if they differed (Table 2). The results showed that the shorelines had equal erosion and accretion over the study duration, therefore site 1 did not have significantly more erosion than site 2 ($p < 0.49$). Both sites had an average negative value, meaning that there was more accretion than erosion (Site 1 = -0.38, Site 2 = -0.42). The shoreline average difference variable was graphed to see the periods of accretion and erosion temporally; the two sites experience periods differently towards the fall season (Figure 8).

Table 2. T-test results with the shoreline average difference variable

	Site 1	***Site 2***
Mean	-0.380456936	-0.42135475
P(T<=t) one-tail	0.496730884	
t Critical one-tail	1.713871528	
P(T<=t) two-tail	0.993461767	
t Critical two-tail	2.06865761	

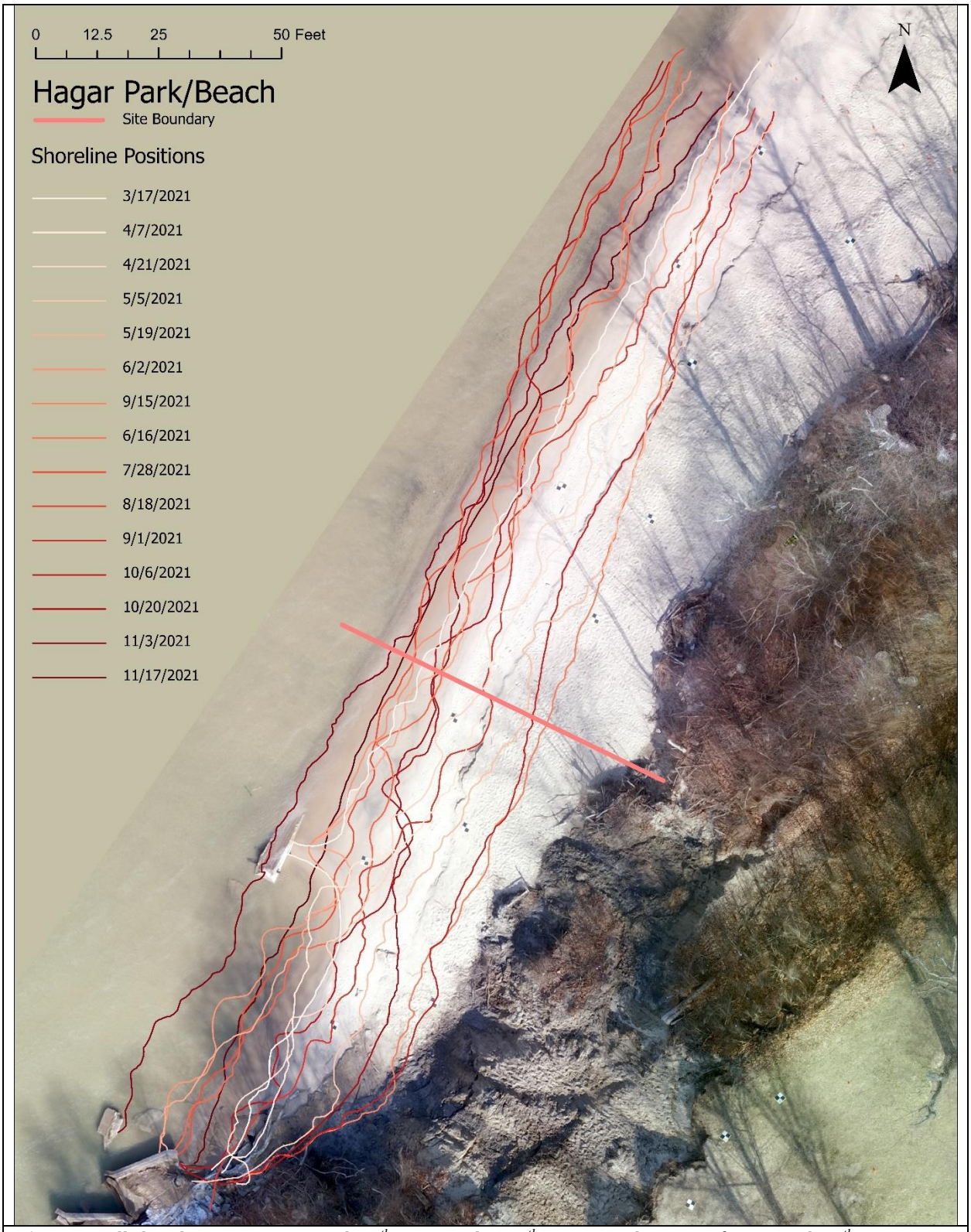

Figure 9. *All shoreline positions, March 17th to November 17th, 2021. Orthomosaic from March 17th, 2021.*

3D Change Analysis

Elevation change is significant during the duration of the study. Point clouds produced by Pix4Dmapper were converted to raster datasets, the raster calculator in ArcGIS Pro, and the color scale modified to highlight changes. Between March 17th and April 7th, there was a significant change in site 1 on the dune, where a portion of it collapsed and increased the elevation of the dune below it (Figure 10a). Both sites have minimal changes along the beach face, except for some moderate decreases in site 2 just before the shoreline. Between April 7th and April 21st, the only changes are moderate decreases just before the shoreline across both sites; however, this does not occur behind the cement foundation (Figure 10b). Between April 21st and May 5th, changes are significant decreases in site 2 just before the shoreline in both sites and evenly on both sites (Figure 10c). Between May 5th and June 2nd, there are moderate increases along the shoreline in both sites and a decrease, then an increase in the area below, on the dune in site 1 (Figure 10d). Between June 2nd and June 16th, there are minimal changes along the beach face (Figure 10e). On the dune in site 1, there is a significant decrease on the dune and a substantial increase below the decrease (Figure 10e). There are similar changes between June 16th and July 28th to the previous survey. However, the decrease in elevation occurs at a higher location, and the increase in elevation is more significant and moved to the shoreline (Figure 10f). Between July 28th and August 18th, there is a moderate decrease along the entire shoreline and a significant reduction just before the toe of the dune in site 1; there are spots of considerable decrease at the top of the dune (Figure 10g). Between August 18th and September 1st, there is only a decrease at the shoreline in site 1 (Figure 10h). Between September 1st and September 15th, there is a substantial decrease at the shoreline in both sites (Figure 10i). Between September 15th and October 6th, there is a significant decrease in elevation between the shoreline

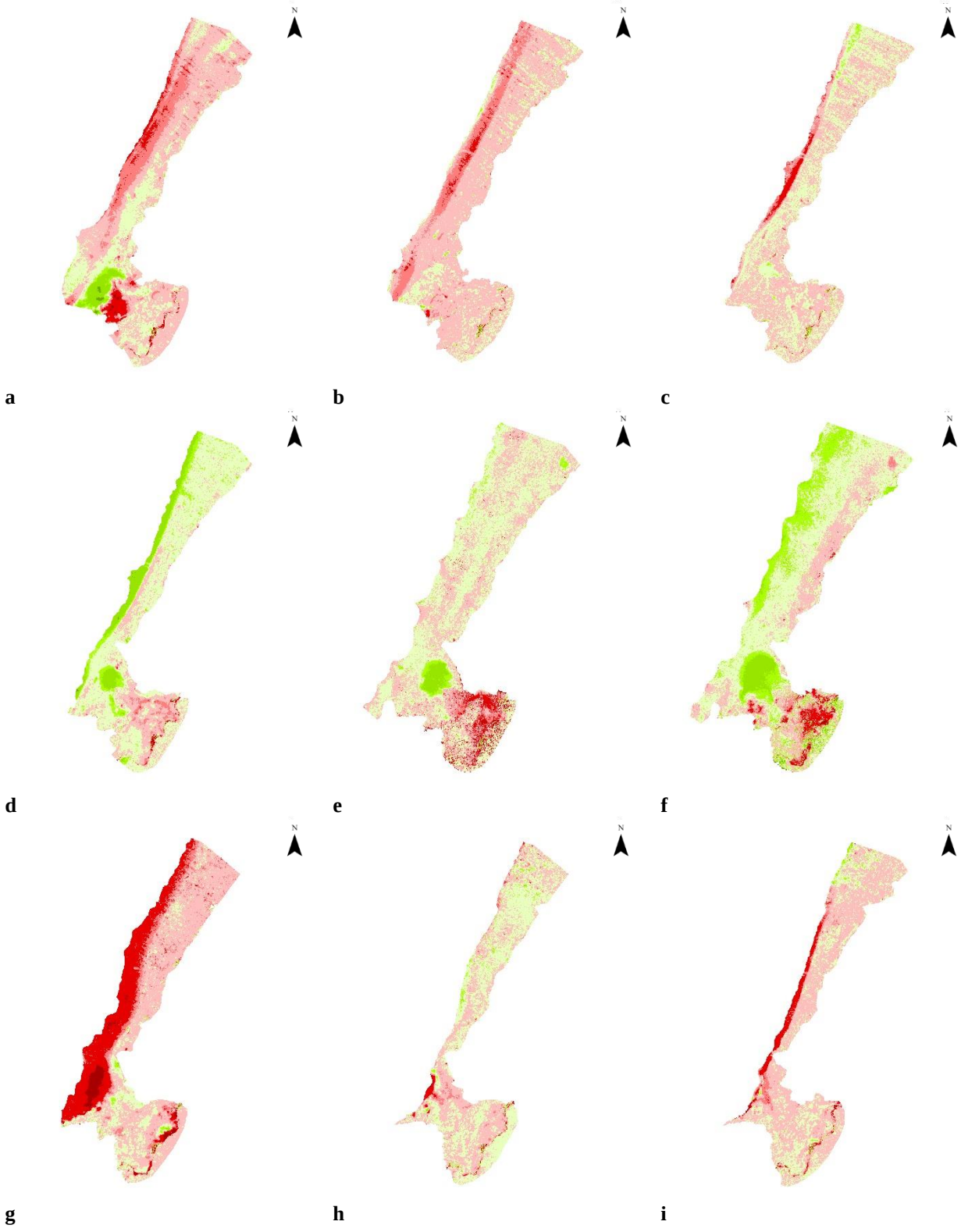
a
b
c
d
e
f
g
h
i

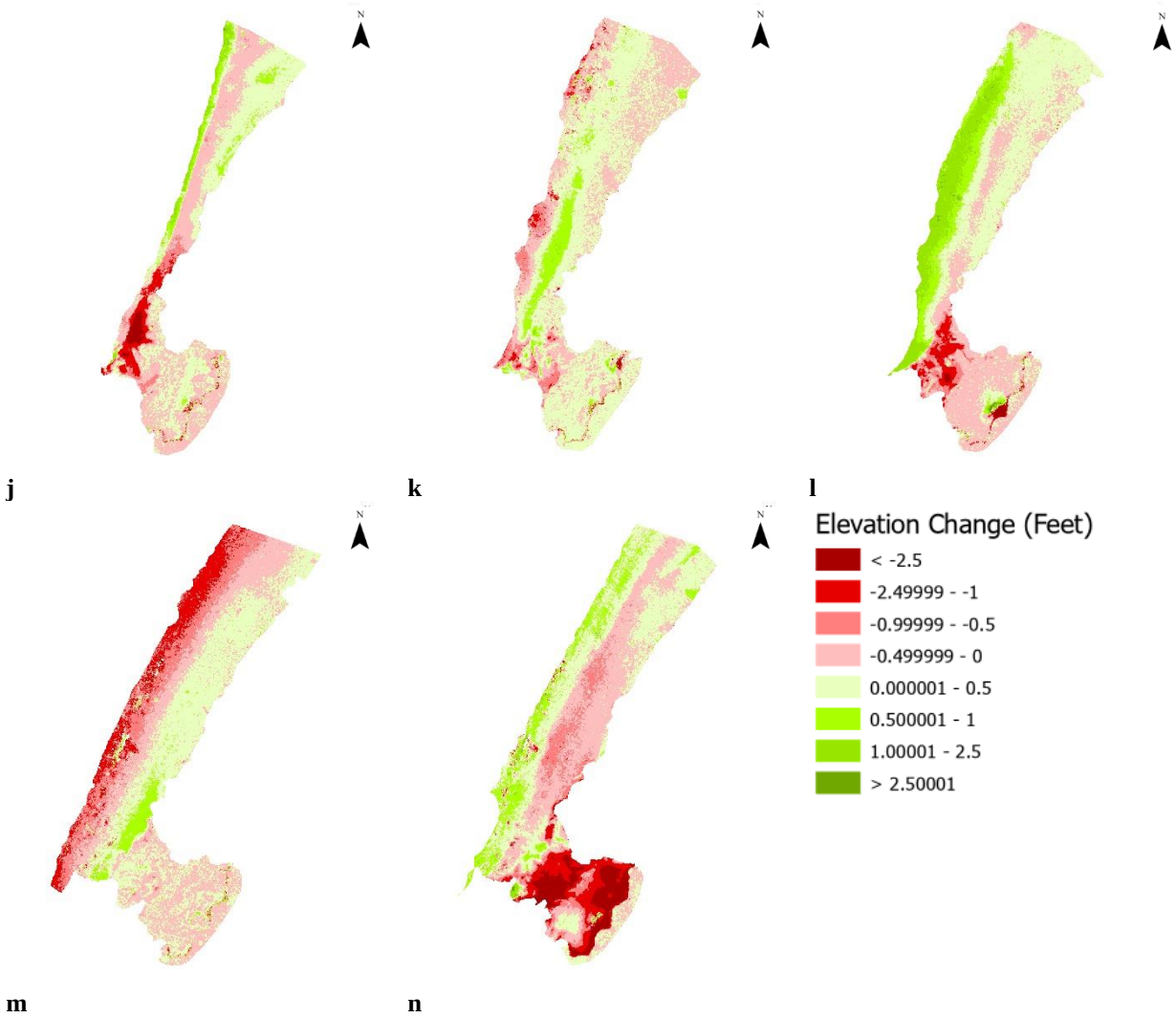

Figure 10. *Raster elevation differences.*

and the toe of the dune (Figure 10j). In parts of site 1 and all of site 2, there is an elevation increase on the shoreline; moving landward, there is a slight elevation decrease (Figure 10j). Between October 6th and October 20th, there are small pockets of elevation that decrease and increase towards the toe of the dune (Figure 10k). Along the beach face, there is a stretch of elevation increase mostly in site 1 part partly in site 2 (Figure 10k). The dune crest collapsed between October 20th and November 3rd, and a subsequent increase below it (Figure 10l). Likewise, at the toe of the dune, there are significant areas of elevation decrease (Figure 10l). There is a considerable elevation increase along the entire study area (Figure 10l). Between

November 3rd and November 11th, there is a moderate elevation increase at the toe of the dune (Figure 10m). Across the whole shoreline, there is an elevation decrease (Figure 10m).

The difference between the first (March 17th, 2021) and the last survey (November 17th, 2021) shows that the most significant elevation decrease is on the dune in Site 1; there are only minimal increases and decreases to elevation on the beach face (Figure 10n). Figure 11 shows the standard deviation of elevation throughout the study; areas that deviate from the mean the most are the toe, crest, and body of the dune; more minor deviations are present on the beach face.

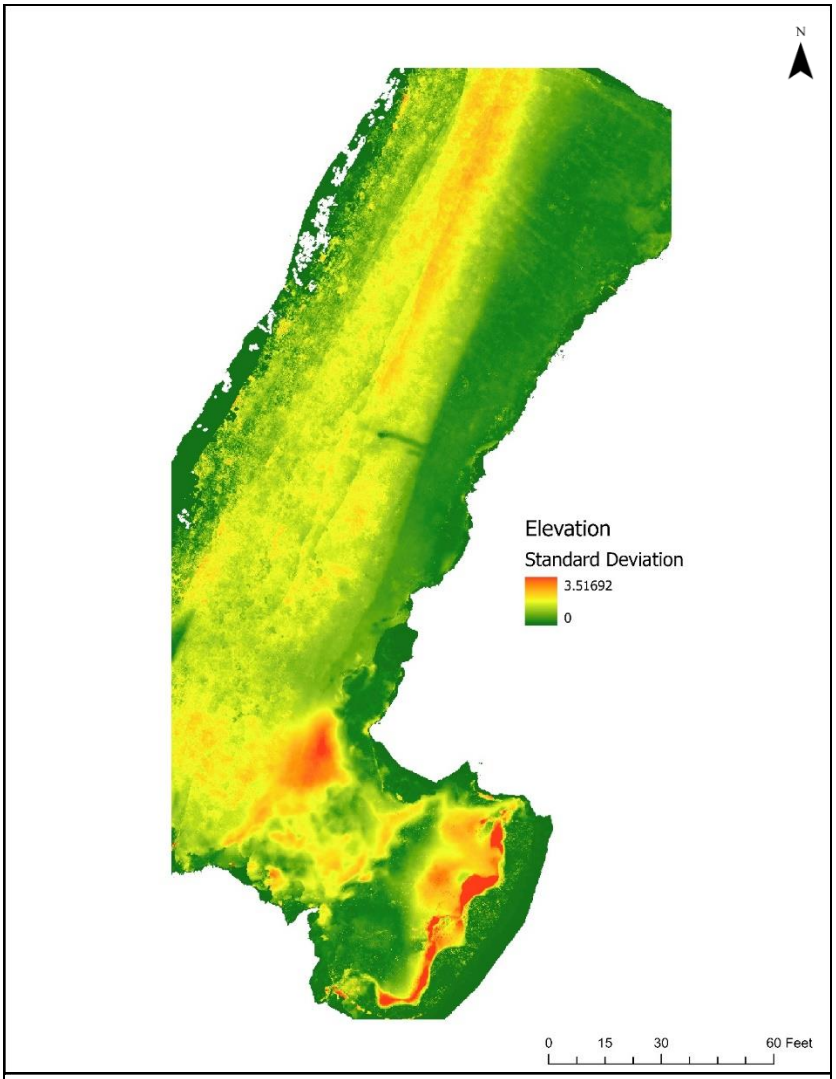

Figure 11. *The standard deviation of elevation using data from all dates.*

DISCUSSION

This study illuminated a high spatial and temporary resolution approach to monitor geomorphic coastal change. UAS-SfM has high potential for research into coastal environments due to its low cost, high spatial and temporal resolution allowing for frequent observations, and its ability to generate both 2D and 3D data for analysis. Hagar Park/Beach was surveyed thirteen times on a biweekly interval over nine months (early spring to late fall). Massive changes in the shoreline and elevation were observed. The shoreline spread was used to place the seawalls' range of influence on the adjacent beach at 205 feet (~62 m) away from the seawall. The shoreline immediately adjacent to the beach experiences the most change, meeting the toe of the dune multiple times over the study period. The wave action onto the toe of the dune is a likely factor decreasing the elevation in the dune (Volpano et al., 2020; Lin et al., 2014; Plant & Griggs, 1992). Due to limitations with the SfM-MVS method, most of the dune at HPB cannot be observed because of the presence of dense vegetation (Volpano et al., 2020; Carrivick, 2016). Thus, the elevation changes on the due immediate to the coastal protections cannot be compared to areas not adjacent or in-between, leaving room for other factors to impact elevation change other than just the seawall. The foot traffic of tourists or heavy rain could move sediment off the dune, thus causing an elevation change. Without observations of the other dune at HPB, the elevation changes of the dune immediately adjacent to the coastal protections cannot be concluded to have been caused by adjacent coastal protections redirecting waves to attack the dune toe.

The finding which supports the 'end-wall' phenomena is the tombolo formation behind the cement foundation immediately adjacent to the coastal protections (Theuerkauf et al., 2019; Balaji et al., 2014). The question of whether seawalls cause more erosion, and their extent of

influence is a question that needs a longer study period to answer. The t-test using the shoreline average difference variable had a slightly higher average in site 1, but it was not significant and within the realm of random chance. It is likely that over a longer period, the erosion in site 1 could be more.

This study conducted research with the UAS-SfM method to explore it applicability for monitoring erosional change adjacent to a seawall. Many considerations could not be included due to time and resource constraints. Future research should take place over several years, including in-situ water level measurements, wave height, and direction to understand their contribution. Waves can crash against the toe of the dune drawing significant amounts of sediment, data on waves and water level could be used to creates rates of erosion. Likewise, linear regression analysis could be used to determine the association between the hydrological variables and erosion. Substantial effort should be put into finding a suitable site to control factors. It is likely the cement wave breakers in between the study area and the seawall dampen the effect of the 'end-wall,' decreasing the potential erosion. Communication with permitting agencies could allow surveying of the site before construction. This was not possible due to the timeframe to complete this study.

To minimize error with the UAS-SfM method, a site with minimal vegetation would be beneficial, as it cannot get the elevation of the surface if dense vegetation is present. For other methods, such as ALS or TLS, this would not be a problem; however, their cost is significantly more (Carrivick, 2016). Likewise, conducting surveys on days with cloud cover would reduce shadows on the site, allows the shoreline to be seen easier, but also limits the vertical error of points present within the shadow. The possibility of real-time monitoring, by mounting a camera in a strategic location on the beach could give insight into the causes of erosion.

CONCLUSION

This study, through repeated surveys conducted over nine months, analyzes shoreline and elevation changes at Hagar Park Beach using high temporal and spatial resolution data. The spread of the shoreline was found dramatically different 205 feet (~62 m) from the seawall. This boundary allows the comparison of the two sites. The difference in shoreline position was measured at multiple points and averaged to create the variable: average shoreline difference. Utilizing a t-test of unequal variances for both sites, it was found that there was not a significant difference between them ($p>.50$). However, the difference between erosional and accretionary periods is evident between the two sites (Figure 7). When one site may be eroding, the other may experience accretion. Nonetheless, we fail to establish a clear influence range of the adjacent seawall because the shoreline average difference becomes equal when averaged over the study duration. Using the 3D results, the most dramatic change is a decrease in elevation occurring on the dune adjacent to the seawall (>1ft). However, the entire dune could not be surveyed due to dense vegetation, thus there is not a 2nd site to compare this elevation change to. There only are minor changes occurring along the beach face (<1ft).

REFERENCES

Balaji, R., S Sathish Kumar, and Ankita Misra. (2017) "Understanding the Effects of Seawall Construction Using a Combination of Analytical Modelling and Remote Sensing Techniques: Case Study of Fansa, Gujarat, India." *The International Journal of Ocean and Climate Systems* 8, no. 3 (June 5, 2017): 153–60. https://doi.org/10.1177/1759313117712180.

Carrivick, J., Smith, M., & Quincey, D. (2016). *Structure from motion in the geosciences*. John Wiley & Sons, Inc.

Conlin, M., Cohn, N., & Ruggiero, P. (2018). A Quantitative Comparison of Low-Cost Structure from Motion (SfM) Data Collection Platforms on Beaches and Dunes. *Journal of Coastal Research*, *34*(6), 1341. https://doi.org/10.2112/jcoastres-d-17-00160.1.

Cook, K. (2017). An evaluation of the effectiveness of low-cost UAVs and structure from motion for geomorphic change detection. *Geomorphology*, *278*, 195–208. https://doi.org/10.1016/j.geomorph.2016.11.009.

Dandois, J. P., & Ellis, E. C. (2010). Remote Sensing of Vegetation Structure Using Computer Vision. *Remote Sensing*, *2*(4), 1157–1176. https://doi.org/10.3390/rs2041157.

Dunford, R., Michel, K., Gagnage, M., Piégay, H., & Trémelo, M.-L. (2009). Potential and constraints of Unmanned Aerial Vehicle technology for the characterization of Mediterranean riparian forest. *International Journal of Remote Sensing*, *30*(19), 4915–4935. https://doi.org/10.1080/01431160903023025.

EGLE. Shoreland Management. 2020a. Michigan Department of Environment, Great Lakes, and Energy. Accessed November 3, 2020. https://www.michigan.gov/egle/0,9429,7-135-3313_3677_3700---,00.html.

EGLE. Shoreline Protection. 2020b. Accessed November 3, 2020. https://www.michigan.gov/egle/0,9429,7-135-3313-164820--,00.html.

ESRI. (n.d.). *2D, 3D & 4D GIS mapping software: ArcGIS Pro*. GIS Mapping Software, Location Intelligence & Spatial Analytics. Retrieved March 8, 2022, from https://www.esri.com/en-us/arcgis/products/arcgis-pro/overview

Favalli, M., Fornaciai, A., Isola, I., Tarquini, S., & Nannipieri, L. (2012). Multiview 3D reconstruction in geosciences. *Computers & Geosciences*, *44*, 168–176. https://doi.org/10.1016/j.cageo.2011.09.012

Fraser, GS, Larsen, CE, and Hester, NC (1990). Climatic control of lake levels in the Lake Michigan and Lake Huron basins. In Late Quaternary History of the Lake Michigan Basin, A.F. Schneider, AF and Fraser, GS (eds). Geological Society of America Special Paper 251: Boulder, Colorado; 75–89.

Hagar/Park Beach. (2020, September 26). [Image]. *Scott P. Fitzgerald*.

Komar, P. D., & McDougal, W. G. (1988). Coastal erosion and engineering structures: the Oregon experience. *Journal of Coastal Research*, 77-92.

Kraus, N. C., & McDougal, W. G. (1996). The effects of seawalls on the beach: Part I, an updated literature review. *Journal of coastal research*, 691-701.

Hartley, R., & Zisserman, A. (2003). Multiple View Geometry in Computer Vision. https://doi.org/10.1017/cbo9780511811685

Harwin, S., & Lucieer, A. (2012). Assessing the Accuracy of Georeferenced Point Clouds Produced via Multi-View Stereopsis from Unmanned Aerial Vehicle (UAV) Imagery. *Remote Sensing*, *4*(6), 1573–1599. https://doi.org/10.3390/rs4061573

James, M. R., & Varley, N. (2012). Identification of structural controls in an active lava dome with high resolution DEMs: Volcán de Colima, Mexico. *Geophysical Research Letters*, *39*(22). https://doi.org/10.1029/2012gl054245.

James, M., & Quinton, J. (2013). Ultra-rapid topographic surveying for complex environments: the hand-held mobile laser scanner (HMLS). *Earth Surface Processes and Landforms*, *39*(1), 138–142. https://doi.org/10.1002/esp.3489.

James, M., & Robson, S. (2012). Straightforward reconstruction of 3D surfaces and topography with a camera: Accuracy and geoscience application. *Journal of Geophysical Research: Earth Surface*, *117*(F3). https://doi.org/10.1029/2011jf002289.

Javernick, L., Brasington, J., & Caruso, B. (2014). Modeling the topography of shallow braided rivers using Structure-from-Motion photogrammetry. *Geomorphology*, *213*, 166–182. https://doi.org/10.1016/j.geomorph.2014.01.006.

Lin, Ying-Tien, and Chin H. Wu. "A Field Study of Nearshore Environmental Changes in Response to Newly-Built Coastal Structures in Lake Michigan." *Journal of Great Lakes Research* 40, no. 1 (March 2014): 102–14. https://doi.org/10.1016/j.jglr.2013.12.013.

Lowe, D. G. (2004). Distinctive Image Features from Scale-Invariant Keypoints. *International Journal of Computer Vision*, *60*(2), 91–110. https://doi.org/10.1023/b:visi.0000029664.99615.94

MacIntosh, K. J., & Anglin, C. D. (1988). ARTIFICIAL BEACH UNITS ON LAKE MICHIGAN. *Coastal Engineering Proceedings*, *1*(21), 211. https://doi.org/10.9753/icce.v21.211

Mancini, F., Dubbini, M., Gattelli, M., Stecchi, F., Fabbri, S., & Gabbianelli, G. (2013). Using Unmanned Aerial Vehicles (UAV) for High-Resolution Reconstruction of Topography:

The Structure from Motion Approach on Coastal Environments. *Remote Sensing*, *5*(12), 6880–6898. https://doi.org/10.3390/rs5126880.

Mathews, A., & Jensen, J. (2012, October). Three-dimensional building modeling using structure from motion: improving model results with telescopic pole aerial photography. In *Proceedings of the 35th Applied Geography Conference, Minneapolis, MN, USA* (pp. 10-12).

Mathews, A., & Jensen, J. (2013). Visualizing and Quantifying Vineyard Canopy LAI Using an Unmanned Aerial Vehicle (UAV) Collected High Density Structure from Motion Point Cloud. *Remote Sensing*, *5*(5), 2164–2183. https://doi.org/10.3390/rs5052164.

McDougal, W. G., Sturtevant, M. A., & Komar, P. D. (1987, May). Laboratory and field investigations of the impact of shoreline stabilization structures on adjacent properties. In *Coastal Sediments* (pp. 961-973). ASCE.

Miles J.R., Russel P.E., Huntley D.A. (2001). Field measurements of sediment dynamics in front of a seawall. J. Coastal Res., 17 (1) (2001), pp. 195-206.

MI Senate. Committee on Environmental Quality. Natural resources and environmental protection act. Bill NO. 714. 3-4. http://www.legislature.mi.gov/documents/2019-2020/billintroduced/Senate/pdf/2020-SIB-0714.pdf

National Research Council (U. S.) Marine Board. Committee on Beach Nourishment and Protection. (1995). *Beach Nourishment and Protection*. Natl Academy Pr.

NOAA. (2018). [Graph]. National Oceanic and Atmospheric Administration. https://www.ndbc.noaa.gov/view_climplot.php?station=45007&meas=wh.

Ouédraogo, M. M., Degré, A., Debouche, C., & Lisein, J. (2014). The evaluation of unmanned aerial system-based photogrammetry and terrestrial laser scanning to generate DEMs of

agricultural watersheds. *Geomorphology*, *214*, 339–355. https://doi.org/10.1016/j.geomorph.2014.02.016.

Pagán, L. Bañón, I. López, C. Bañón, L. Aragonés, Monitoring the dune-beach system of Guardamar del Segura (Spain) using UAV, SfM and GIS techniques, Science of The Total Environment, Volume 687, 2019, Pages 1034-1045, ISSN 0048-9697, https://doi.org/10.1016/j.scitotenv.2019.06.186.

Papakonstantinou, A., Topouzelis, K., & Pavlogeorgatos, G. (2016). Coastline Zones Identification and 3D Coastal Mapping Using UAV Spatial Data. *ISPRS International Journal of Geo-Information*, *5*(6), 75. https://doi.org/10.3390/ijgi5060075.

Pix4D. (2020). [Image]. https://support.pix4d.com/hc/en-us/articles/115002471546-Image-acquisition.

Pix4D. (n.d.a). How to include GCPs in the project. https://support.pix4d.com/hc/en-us/articles/202560239-How-to-include-GCPs-in-the-project.

Pix4D. (2020b). *Step 1. Before Starting a Project > 1. Designing the Image Acquisition Plan > a. Selecting the Image Acquisition Plan Type*. A Project from A to Z. https://support.pix4d.com/hc/en-us/articles/202557459-Step-1-Before-Starting-a-Project-1-Designing-the-Image-Acquisition-Plan-a-Selecting-the-Image-Acquisition-Plan-Type#label5.

Plant, N.G, Griggs G.B (1992). Interaction between nearshore processes and beach morphology near a seawall. J. Coastal Res., 8 (1) (1992), pp. 183-200

Plets, G., Gheyle, W., Verhoeven, G., De Reu, J., Bourgeois, J., Verhegge, J., & Stichelbaut, B. (2012). Three-dimensional recording of archaeological remains in the Altai Mountains. *Antiquity*, *86*(333), 884–897. https://doi.org/10.1017/s0003598x00047980

Rossi, R., Buscombe, D., Grams, P. E., Schmidt, J. C., & Wheaton, J. M. (2016, December). From Hype to an Operational Tool: Efforts to Establish a Long-Term Monitoring Protocol of Alluvial Sandbars using Structure-from-Motion' Photogrammetry. In *AGU Fall Meeting Abstracts* (Vol. 2016, pp. EP21D-0916).

Ruggiero, P., Kaminsky, G. M., Gelfenbaum, G., & Voigt, B. (2005). Seasonal to Interannual Morphodynamics along a High-Energy Dissipative Littoral Cell. *Journal of Coastal Research, 213*, 553–578. https://doi.org/10.2112/03-0029.1.

Sagan, C., Soter, S., & Druyan, A. (1980). Cosmos: A Personal Voyage. Episode 1.

Simon. (2015). *DJI Inspire 1 quadcopter*. Drone Doctor UK. Retrieved March 7, 2022, from https://www.dronedoctor.co.uk/dji-inspire-1-07/

Smith, M. J., Chandler, J., & Rose, J. (2009). High spatial resolution data acquisition for the geosciences: kite aerial photography. *Earth Surface Processes and Landforms*, *34*(1), 155–161. https://doi.org/10.1002/esp.1702.

Snavely, N., Seitz, S. M., & Szeliski, R. (2008). Modeling the World from Internet Photo Collections. *International Journal of Computer Vision*, *80*(2), 189–210. https://doi.org/10.1007/s11263-007-0107-3

Steven M. Colman, Richard M. Forester, Richard L. Reynolds, Donald S. Sweetkind, John W. King, Paul Gangemi, Glenn A. Jones, Lloyd D. Keigwin, David S. Foster, Lake-Level History of Lake Michigan for the Past 12,000 Years: The Record From Deep Lacustrine Sediments, Journal of Great Lakes Research, Volume 20, Issue 1, 1994, Pages 73-92, ISSN 0380-1330, https://doi.org/10.1016/S0380-1330(94)71133-3.

Sturdivant, Emily, Erika Lentz, E. Robert Thieler, Amy Farris, Kathryn Weber, David Remsen, Simon Miner, and Rachel Henderson. “UAS-SfM for Coastal Research: Geomorphic

Feature Extraction and Land Cover Classification from High-Resolution Elevation and Optical Imagery." Remote Sensing 9, no. 10 (September 3, 2017): 1020. https://doi.org/10.3390/rs9101020.

Szeliski, R. (2011). Computer Vision: Algorithms and Applications. *Texts in Computer Science*. https://doi.org/10.1007/978-1-84882-935-0.

Theuerkauf, Ethan J., Katherine N. Braun, Danielle M. Nelson, Morgan Kaplan, Salvatore Vivirito, and Jack D. Williams. "Coastal Geomorphic Response to Seasonal Water-Level Rise in the Laurentian Great Lakes: An Example from Illinois Beach State Park, USA." *Journal of Great Lakes Research* 45, no. 6 (December 2019): 1055–68. https://doi.org/10.1016/j.jglr.2019.09.012.

Thoeni, K., Giacomini, A., Murtagh, R., & Kniest, E. (2014). A comparison of multi-view 3D reconstruction of a rock wall using several cameras and a laser scanner. *ISPRS - International Archives of the Photogrammetry, Remote Sensing and Spatial Information Sciences*, *XL-5*, 573–580. https://doi.org/10.5194/isprsarchives-xl-5-573-2014.

Triggs, B., McLauchlan, P. F., Hartley, R. I., & Fitzgibbon, A. W. (2000). Bundle Adjustment — A Modern Synthesis. *Vision Algorithms: Theory and Practice*, 298–372. https://doi.org/10.1007/3-540-44480-7_21.

Tsai, M. L., Chiang, K. W., Huang, Y. W., Lin, Y. S., Tsai, J. S., Lo, C. F., ... & Wu, C. H. (2010, June). The development of a direct georeferencing ready UAV based photogrammetry platform. In *Proceedings of the 2010 Canadian Geomatics Conference and Symposium of Commission I*.

Turner, D., Lucieer, A., & Wallace, L. (2013). Direct georeferencing of ultrahigh-resolution UAV imagery. *IEEE Transactions on Geoscience and Remote Sensing*, *52*(5), 2738-2745.

Turner, I. L., Harley, M. D., & Drummond, C. D. (2016). UAVs for coastal surveying. *Coastal Engineering*, *114*, 19–24. https://doi.org/10.1016/j.coastaleng.2016.03.011.

U.S. Army Corps of Engineers (2020). Great Lakes Water Level Data. https://www.lre.usace.army.mil/Missions/Great-Lakes-Information/Great-Lakes-Information-2/Water-Level-Data/.

USGS. "Digital Shoreline Analysis System (DSAS)." *Digital Shoreline Analysis System (DSAS) U.S. Geological Survey*, U.S., 4 Oct. 2018, https://www.usgs.gov/centers/whcmsc/science/digital-shoreline-analysis-system-dsas?qt-science_center_objects=6#qt-science_center_objects.

Vericat, D., Múñoz-Narciso, E., Béjar, M., & Ramos-Madrona, E. (2016). Case study: Multitemporal reach-scale topographic models in a wandering river-uncertainties and opportunities. *Structure from Mofion in the Geosciencies. New Analyfical Methods in the Earth Environmental Science*.

Volpano, C. A., Zoet, L. K., Rawling, J. E., Theuerkauf, E. J., & Krueger, R. (2020). Three-dimensional bluff evolution in response to seasonal fluctuations in Great Lakes water levels. *Journal of Great Lakes Research*, *46*(6), 1533–1543. https://doi.org/10.1016/j.jglr.2020.08.017

Westoby, M. J., Brasington, J., Glasser, N. F., Hambrey, M. J., & Reynolds, J. M. (2012). 'Structure-from-Motion' photogrammetry: A low-cost, effective tool for geoscience applications. *Geomorphology*, *179*, 300–314. https://doi.org/10.1016/j.geomorph.2012.08.021.

Westoby, M. J., Lim, M., Hogg, M., Pound, M. J., Dunlop, L., & Woodward, J. (2018). Cost-effective erosion monitoring of coastal cliffs. *Coastal Engineering*, *138*, 152–164. https://doi.org/10.1016/j.coastaleng.2018.04.008

Zimmerman, T., Jansen, K., & Miller, J. (2020). Analysis of UAS Flight Altitude and Ground Control Point Parameters on DEM Accuracy along a Complex, Developed Coastline. *Remote Sensing*, *12*(14), 2305. http://dx.doi.org/10.3390/rs12142305.